Switching Control between 3-coil and 5-coil modes for 6-pole Active Magnetic Bearings

Satoshi Ueno [a], Masayuki Chiba [a], Changan Jiang [a]

[a] Ritsumeikan University, 1-1-1 Nojihigashi, Kusatsu, Shiga, Japan, sueno@se.ritsumei.ac.jp

***Abstract*—6-pole active magnetic bearings (AMBs) have fewer poles than usual 8-pole AMBs, then, it is easier to miniaturize and suitable for small motors. In this paper, we propose the novel control method for the 6-coil AMB, which switches between 3-coil and 5-coil modes. The 3-coil mode uses three coils to generate bearing force and can reduce power consumption. On the other hand, the 5-coil mode uses five coils, and can generate larger maximum force than that of the 3-coil mode. By switching between the two modes, it is possible to realize both lower power consumption and larger bearing force. This paper introduces the coil currents in the 5-coil mode and shows the results of levitation and rotation tests. The results show that the proposed method realizes stable levitation with lower current limit compared with other methods.**

I. Introduction

Recently, the demands for improving the durability and reducing the noise of small motors have been considerably increasing. Therefore, magnetically suspended motors have been developed [1-4]. They have advantages such as no friction loss, no abrasion, and lubrication-free operation. Furthermore, active magnetic bearings (AMBs) have the advantage of vibration suppression and high-performance control because it is capable of active control. Then the development of a smaller and relatively low cost AMB is desired, and we have developed a 6-pole AMB [5-10]. Since 6-pole AMBs have fewer poles than usual 8-pole AMBs, it is easier to miniaturize and reduce costs. However, because the magnetic circuit of the 6-pole AMBs is difference in the x- and y-directions, the calculation of coil currents becomes complex. We have developed several control methods such as a minimum energy control method [7], a maximum bearing force control method [8], etc.

The minimum energy control method uses three coils located near the direction of target bearing force. We call this method a 3-coil mode in this paper. This method can reduce copper losses, however, the maximum bearing force towards a pole becomes 72 % of the maximum bearing force towards the center of two poles. To solve this problem, the maximum bearing force control method has been developed. This method uses five coils, and three coils in the middle are supplied the same magnitude currents while two coils on sides control the direction of the bearing force. In this method, almost the same maximum bearing force can be obtained in all directions. However, this method needs more energy than that of the 3-coil mode [10].

In this paper, to realize both low power consumption and large maximum force, we introduce a switching control method. When the bearing force is small, the coils are driven by the 3-coil mode. If one of the coil currents reaches a limit value, the coil currents are switched to the 5-coil mode. To realize a smooth switching, a new calculation method in the 5-coil mode are developed instead of the maximum bearing force control method.

In this paper, the coil currents are derived in the 3- and 5-coil modes. The proposed method is verified by numerically simulations and experiments. The results show that the proposed method realizes stable levitation with lower current limit compared with other methods.

II. Control Method

A. Bearing Force of 6-pole AMB

A coordinate system is shown in Fig. 1. Stator poles are located and numbered as shown in the figure. $i_{1\sim6}$ are currents of each coil and $B_{1\sim6}$ are magnetic flux densities at the air gap between stator poles and rotor. The sum of B_k is zero. Magnetic attractive force at each pole is expressed as

$$f_k = \frac{S}{2\mu_0} B_k^2 \tag{1}$$

where μ_0 is the permeability of air, S is the cross section of the pole and k is the ordinal number of the poles. x- and y-directional forces are calculated as

$$f_x = \frac{\sqrt{3}}{2}(f_6 + f_5 - f_2 - f_3) \tag{2}$$

$$f_y = f_1 + \frac{1}{2}f_2 - \frac{1}{2}f_3 - f_4 - \frac{1}{2}f_5 + \frac{1}{2}f_6 \tag{3}$$

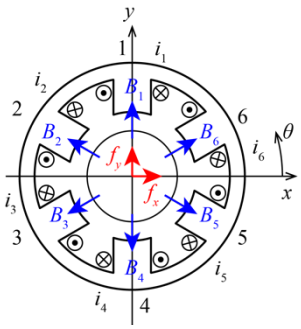

Figure 1. Coordinate system of 6-pole AMB.

B. Calculation of Magnetic Flux Density in 3-Coil Mode

In case of the 3-coil mode, only three poles in the neighborhood of the angle of target force are used. For example, if the target angle is from 60° to 120°, pole 6, 1 and 2 are used,

then $B_3 = B_4 = B_5 = 0$. Therefore, the magnetic flux densities are obtained by solving the following simultaneous equations.

$$\hat{f}_x = \frac{\sqrt{3}S}{4\mu_0}(B_6^2 - B_2^2) \tag{4}$$

$$\hat{f}_y = \frac{S}{2\mu_0}\left(B_1^2 + \frac{1}{2}B_2^2 + \frac{1}{2}B_6^2\right) \tag{5}$$

$$B_1 + B_2 + B_6 = 0 \tag{6}$$

where $\hat{f}_x$ and $\hat{f}_y$ are target forces. The solution becomes

$$B_k = (-1)^{k-1}\sqrt{\frac{4\mu_0}{5\sqrt{3}S}}\sqrt{\hat{f}}\, f_A\left(\hat{\phi} - \frac{k-1}{3}\pi\right) \tag{7}$$

$$f_A(\psi) = \begin{cases} \sqrt{\sqrt{13}\cos(\psi + \alpha_1) - \beta_1} & 0° \le \psi < 60° \\ \sqrt{\sqrt{3}\sin\psi + \beta_2} & 60° \le \psi < 120° \\ \sqrt{-\sqrt{13}\cos(\psi + \alpha_3) - \beta_3} & 120° \le \psi < 180° \\ 0 & 180° \le \psi < 360° \end{cases}$$

$$\alpha_1 = \tan^{-1}\left(\frac{3\sqrt{3}}{5}\right) - \frac{2\pi}{3}$$

$$\alpha_3 = \tan^{-1}\left(\frac{3\sqrt{3}}{5}\right) + \frac{2\pi}{3}$$

$$\beta_1 = \sqrt{-4\cos\left(2\psi + \frac{2\pi}{3}\right) - 1}$$

$$\beta_2 = \sqrt{-4\cos(2\psi) - 1}$$

$$\beta_3 = \sqrt{-4\cos\left(2\psi - \frac{2\pi}{3}\right) - 1}$$

where $\hat{f}$ and $\hat{\phi}$ are the magnitude and angle of the target force. When B_k are less than the maximum value, the target force can be obtained.

C. Calulation of Magnetic Flux Density in 5-coil Mode

When one of the magnetic flux density of poles reaches to its maximum, further two poles can be utilized to produce larger force. Here, the target angle of $60° \le \hat{\phi} \le 120°$ is considered. In this case, pole 5, 6, 1, 2 and 3 are used, and pole 1 reaches to its maximum magnetic flux density $B_{\max}$.

Since B_1 is maximum, the force at pole 1 becomes

$$\bar{f}_1 = \frac{S}{2\mu_0}B_{\max}^2 \tag{8}$$

Then the AMB has to produce the rest of force by using pole 2, 3, 5 and 6, and the following relationships are derived.

$$\hat{f}_x = \frac{\sqrt{3}}{2}\{(f_6 - f_3) + (f_5 - f_2)\} \tag{9}$$

$$\hat{f}_y - \bar{f}_1 = \frac{1}{2}\{(f_6 - f_3) - (f_5 - f_2)\} \tag{10}$$

From equations (9) and (10), we have

$$f_6 - f_3 = \frac{1}{\sqrt{3}}\hat{f}_x + \hat{f}_y - \bar{f}_1 \tag{11}$$

$$f_5 - f_2 = \frac{1}{\sqrt{3}}\hat{f}_x - \hat{f}_y + \bar{f}_1 \tag{12}$$

On the other hand, the forces produced by the couple of opposite poles are expressed as

$$f_6 - f_3 = \frac{S}{2\mu_0}(B_6 + B_3)(B_6 - B_3) = \frac{2S}{\mu_0}B_{b63}B_{c63} \tag{13}$$

$$f_5 - f_2 = \frac{S}{2\mu_0}(B_5 + B_2)(B_5 - B_2) = \frac{2S}{\mu_0}B_{b52}B_{c52} \tag{14}$$

where

$$B_{b63} = \frac{B_6 + B_3}{2}, \qquad B_{c63} = \frac{B_6 - B_3}{2}$$

$$B_{b52} = \frac{B_5 + B_2}{2}, \qquad B_{c52} = \frac{B_5 - B_2}{2}$$

and

$$B_6 = B_{b63} + B_{c63}, \qquad B_3 = B_{b63} - B_{c63}$$

$$B_5 = B_{b52} + B_{c52}, \qquad B_2 = B_{b52} - B_{c52}$$

Therefore, B_{c63} and B_{c52} are calculated as

$$B_{c63} = \frac{\mu_0}{2S}\frac{1}{B_{b63}}\left(\frac{1}{\sqrt{3}}\hat{f}_x + \hat{f}_y - \bar{f}_1\right) \tag{15}$$

$$B_{c52} = \frac{\mu_0}{2S}\frac{1}{B_{b52}}\left(\frac{1}{\sqrt{3}}\hat{f}_x - \hat{f}_y + \bar{f}_1\right) \tag{16}$$

Next, we have to determine B_{b63} and B_{b52}. Since $B_4 = 0$, the magnetic flux densities satisfy the following relation.

$$B_2 + B_3 + B_5 + B_6 = 2(B_{b63} + B_{b52}) = -B_{\max} \tag{17}$$

Then we have

$$B_{b63} = -\frac{1}{2}B_{\max} - B_{b52} \tag{18}$$

Next, B_{b52} is discussed. When B_1 reaches to $B_{\max}$ with the 3-coil mode, B_2 and B_6 are calculated as

$$B_2 = B_{\max}f_B(\hat{\phi}) \tag{19}$$

$$B_6 = -B_{\max} - B_2 \tag{20}$$

$$f_B(\psi) = \begin{cases} 0 & \psi = 60° \\ -\frac{1}{2}\gamma_1 & 60° < \psi < 90° \\ -\frac{1}{2} & \psi = 90° \\ -\frac{1}{2}\gamma_2 & 90° < \psi < 120° \\ -1 & \psi = 120° \end{cases} \tag{21}$$

$$\gamma_1 = 1 - \sqrt{3}\tan\psi + \sqrt{3\tan^2\psi - 5}$$

$$\gamma_2 = 1 - \sqrt{3}\tan\psi - \sqrt{3\tan^2\psi - 5}$$

In this case, B_5 and B_3 are zero, and then we have

$$B_{b52} = \frac{1}{2}B_2 \tag{22}$$

$$B_{b63} = \frac{1}{2}B_6 = \frac{1}{2}(-B_{\max} - B_2) \tag{23}$$

Therefore, we can determine B_{b52} and B_{b63}.

The other directions can be calculated by using coordinate transformation.

D. Coil Currents

A magnetic circuit of a 6-pole AMB is shown in Fig. 2. N is the number of coil turns, and $R_{1\sim6}$ are magnetic resistance of air gap and represented by

$$R_k = \frac{1}{\mu_0 S}\left(g_0 + x\sin\frac{(k-1)\pi}{3} - y\cos\frac{(k-1)\pi}{3}\right) \tag{24}$$

From the magnetic circuit the following equation is derived.

$$\mathbf{RB} = \frac{N}{S}\mathbf{Ci} \tag{25}$$

where

$$\mathbf{R} = \begin{bmatrix} R_1 & -R_2 & 0 & 0 & 0 \\ 0 & R_2 & -R_3 & 0 & 0 \\ 0 & 0 & R_3 & -R_4 & 0 \\ 0 & 0 & 0 & R_4 & -R_5 \\ R_6 & R_6 & R_6 & R_6 & R_5 + R_6 \end{bmatrix}$$

$$\mathbf{C} = \begin{bmatrix} 1 & -1 & 0 & 0 & 0 & 0 \\ 0 & 1 & -1 & 0 & 0 & 0 \\ 0 & 0 & 1 & -1 & 0 & 0 \\ 0 & 0 & 0 & 1 & -1 & 0 \\ 0 & 0 & 0 & 0 & 1 & -1 \end{bmatrix}$$

$$\mathbf{B} = [B_1 \quad B_2 \quad B_3 \quad B_4 \quad B_5]^T$$

$$\mathbf{i} = [i_1 \quad i_2 \quad i_3 \quad i_4 \quad i_5 \quad i_6]^T$$

Then the coil currents are obtained by

$$\mathbf{i} = \frac{S}{N}\mathbf{C}^{+}\mathbf{RB} \tag{26}$$

where $\mathbf{C}^{+}$ is pseudo-inverse of $\mathbf{C}$. If the displacements are small and can be neglected, the coil currents are calculated by

$$i_k = \frac{g_0}{\mu_0 N}B_k \tag{27}$$

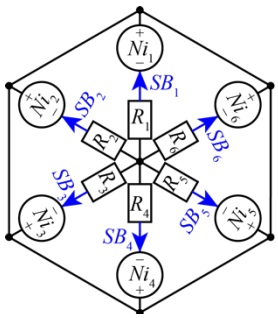

Figure 2. Magnetic circuit of 6-pole AMB.

E. Implementation

To reduce computation time, $f_A(\psi)$ and $f_B(\psi)$ are calculated beforehand and stored in Lookup Tables.

Firstly, the target forces $\hat{f}_x$ and $\hat{f}_y$ are transformed to $\hat{f}$ and $\hat{\phi}$. Then the coil currents are calculated by the 3-coil mode and compared with their limit value. If the maximum of the coil currents is less than the limit value, the controller outputs the currents in the 3-coil mode. If the currents are over the limit, the calculation method is switched to the 5-coil mode.

In the 5-coil mode, B_{b52} and B_{b63} are firstly calculated by equations (22) and (23), and then B_{c52} and B_{c63} are calculated by equations (15) and (16).

F. Numerical Verification

The proposed method was verified numerically. The parameters are shown in Table 1, which are the same as the experimental device described later. The displacement of the rotor was fixed to zero, and the limit of the coil current was set to 0.2 A. In this case, $B_{\max}$ is 0.34 T, and $\bar{f}$ is 1.84 N.

Figure 3 shows the results of that the magnitude of target force was changed from 0 to maximum while the target angle was set to 105 degrees. The upper graph shows the coil currents, while the lower graph shows the resultant magnitude and angle of the bearing force. When the target magnitude is smaller than the maximum value of the 3-coil mode, the currents of coil 3, 4 and 5 are zero. When the target force is over the maximum value of the 3-coil mode, the currents of coil 3 and 5 are supplied and the larger force is obtained.

Figure 4 shows the results of that the target angle was changed from 60 to 120 degrees with the fixed magnitude of 2.7 N. From about 65 to 113 degrees, the coil currents switch to the 5-coil mode.

The coil currents change without leap from the 3-coil mode to the 5-coil mode in both cases.

Figure 5 shows the results of the bearing force at current limit with the 3- and 5-coil modes. By using the 5-coil mode, larger force is obtained. Dashed lines indicate the inscribed circles of each mode. The radius of the 5-coil mode is 137% of that of the 3-coil mode.

TABLE I. PARAMETERS OF 6-POLE AMB

g_0	Air gap	0.222×10^{-3}	m
S	Cross section	$4 \times 10 \times 10^{-6}$	m^2
N	Coil turns	300	

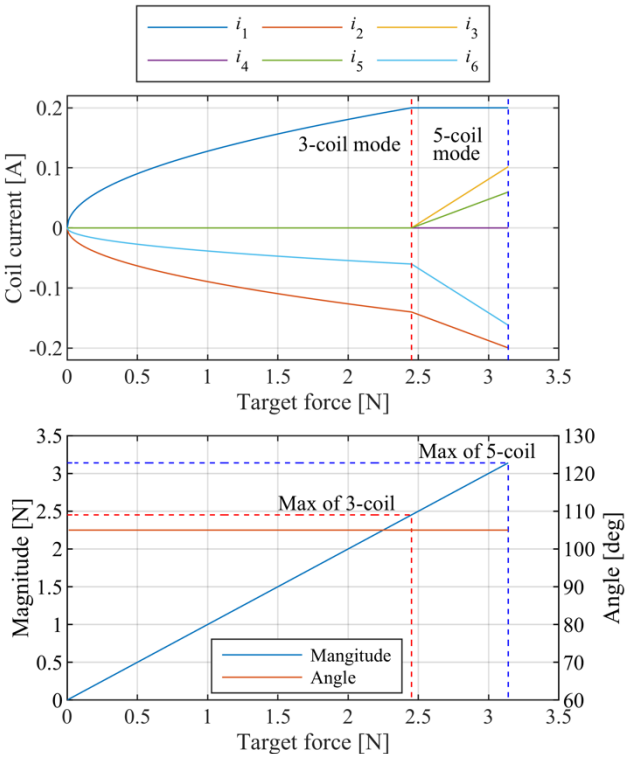

Figure 3. Coil currents and bearing force from 0 to maximum magnitude with fixed angle of 105 degrees.

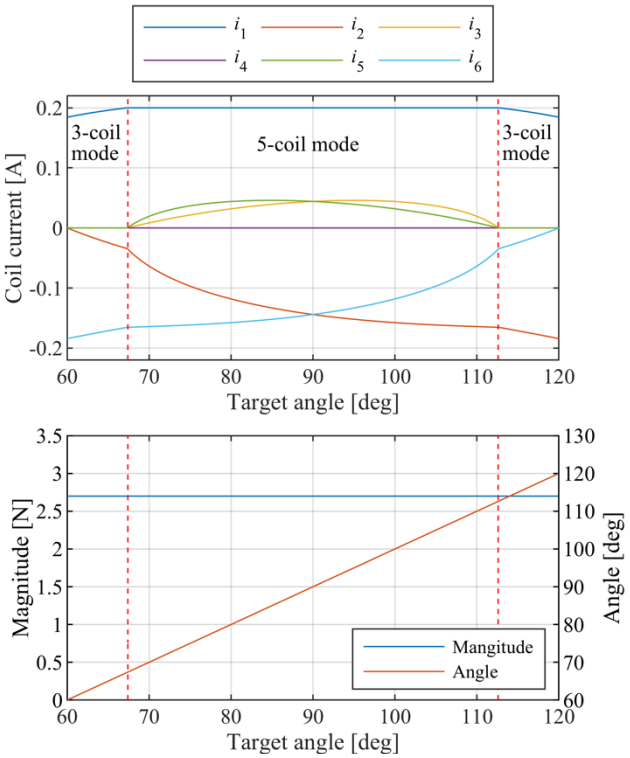

Figure 4. Coil currents and bearing force from 60 to 120 degrees with fixed magntidue of 2.7 N.

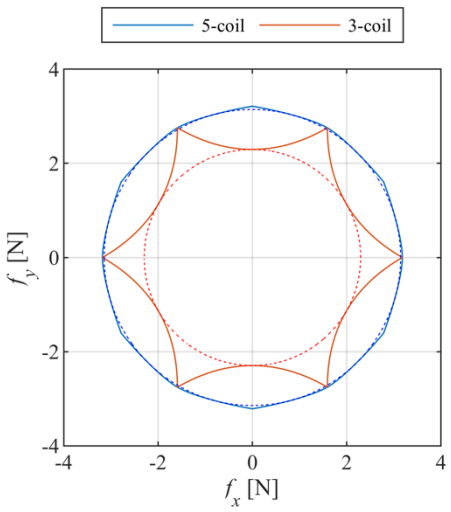

Figure 5. Bearing force at current limit.

III. Experimental Verifcation

A. AMBs-Motor Device

A test device is shown in Fig. 6. A rotor is set horizontally and 6-pole AMBs are placed on each side of the rotor. A three-phase permanent magnet synchronous motor (PMSM) is installed in the middle of the rotor. A thrust magnetic bearing is not used, and the passive stability of the PMSM is used to support the rotor along the axial axis. The dimensions of the test device are shown in Table II. The stators of the AMB and PMSM are the same specifications except for coils. The total weight of the rotor is 38 g, which is too light for a capacity of AMBs. Hence the current limit was reduced from usual value.

Four displacement sensors are installed on the outside of the AMBs to detect the displacement of the rotor. Eddy current type displacement sensors (Omron: ZX-EDR5) are adopted.

A control system is shown in Fig. 7. A digital signal processor (DSP, mtt: Lory Accel) is used for control. The DSP reads the displacement signals via A/D converters and calculates the coil currents of the AMBs and PMSM. Then the DSP outputs the current commands via D/A converters to power amplifiers. The power amplifiers adopt Power Op Amps (TI, OPA548), and supply current to the coils.

TABLE II. Specifications of Test Device

Stator outer diameter	ϕ 38 mm
Stator inner diameter	ϕ 10.5 mm
Rotor outer diameter	ϕ 10.1 mm
Thickness	10 mm
Martial	Silicon steel (t = 0.5 mm)
AMB coil	UEW, ϕ 0.1 mm × 300 turns, 20 Ω
Motor PM	Neodymium, cylindrical shape, ϕ 8 mm × ϕ 5 mm × 10 mm, radial 2-pole magnetization
Motor coil	UEW, ϕ 0.14 mm × 170 turns, 8 Ω

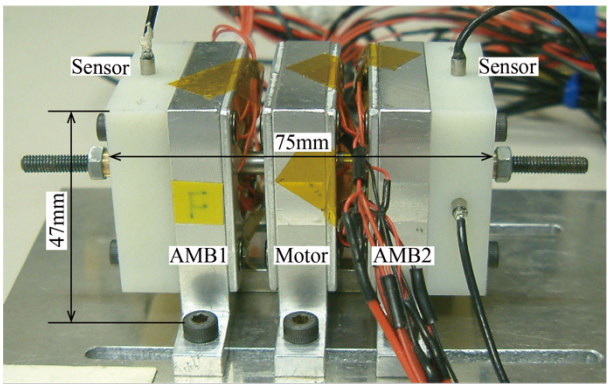

(a) AMB-Motor device

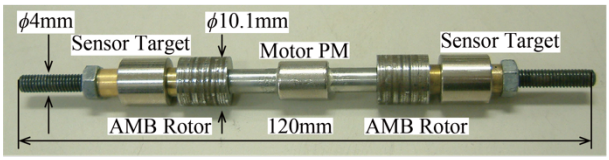

(b) Rotor

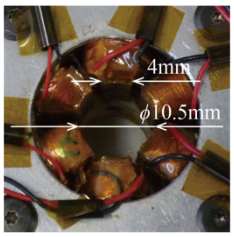

(c) Stator

Figure 6. Photographs of AMB-Motor device, rotor and stator.

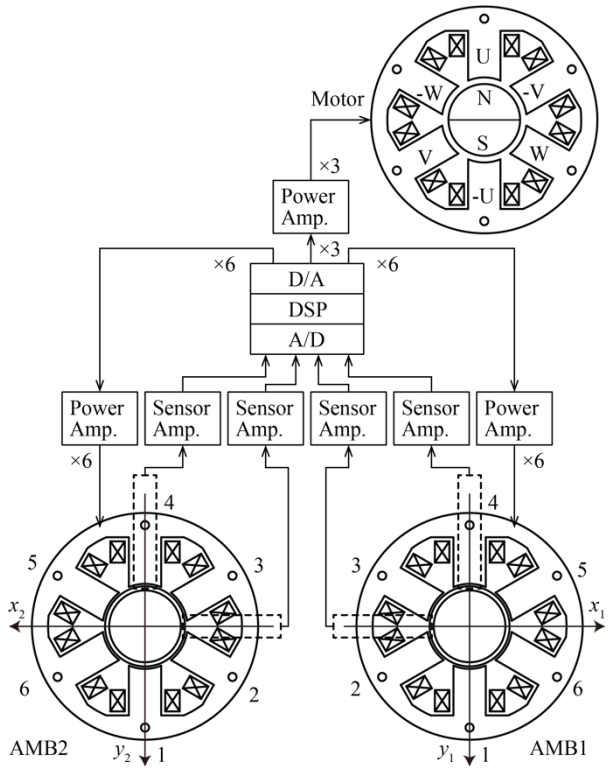

Figure 7. Control system.

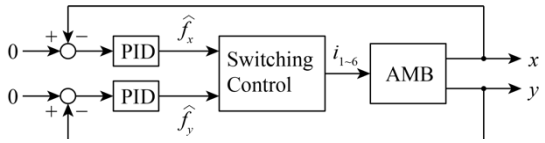

Figure 8. Controller for single AMB.

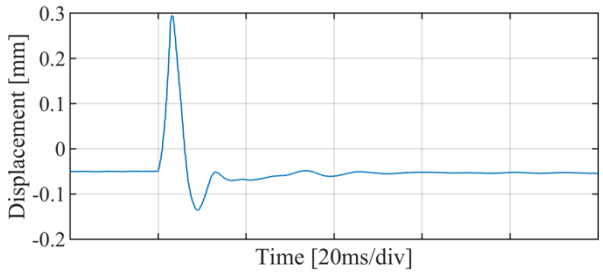

Figure 9. Impulse resonse in y-axis of AMB1 with switching controller. P-, D- and I-gains were 23 N/mm, 0.032 Ns/mm and 0 N/mms, respectively.

Figure 8 shows the controller of single AMB. PID controllers are adopted for the position control. Each coil currents of the 6-pole AMBs are calculated by the switching control method from the output of the PID controllers. The gains of the PID controllers were experimentally determined.

The PMSM is driven by three-phase current with constant magnitude. Rotational speed is controlled by the frequency of the three-phase current.

B. Results

Levitation and rotation tests were carried out. In the test, the current limit was reduced to small value, in which case the rotor could not levitate by the 3-coil mode.

Figure 9 shows the impulse response in y-axis of AMB1 while levitation. This result confirms the stable levitation could be achieved with the switching controller.

Figure 10 show the displacement and coil current while levitation. Figure 10 (a) is the results of AMB1 which currents were limited to 0.2 A, while (b) is the results of AMB2 which currents are limited to 0.1 A. The AMB1 was controlled by 3-coil mode, while the AMB2 was controlled by 5-coil mode. These results confirm the 5-coil mode was working well.

The rotation test was carried out with the current limit of 0.115 A in both the AMBs, and the rotor could rotate up to 55,000 rpm. Figure 11 shows the amplitude of oscillation. For comparison, the results with the minimum energy controller and maximum force controller were shown. Because these controllers could not realize stable levitation with the same current limit as the switching controller, larger current limit was adopted. The amplitude level of the switching control is almost the same as other controllers. Figure 12 shows the power consumption of the AMBs. The switching controller resulted in maximum power consumption. In the switching controller, lower current limit was adopted, then the coil currents were close to their limit value. Therefore, the power consumption increased compared with other controllers.

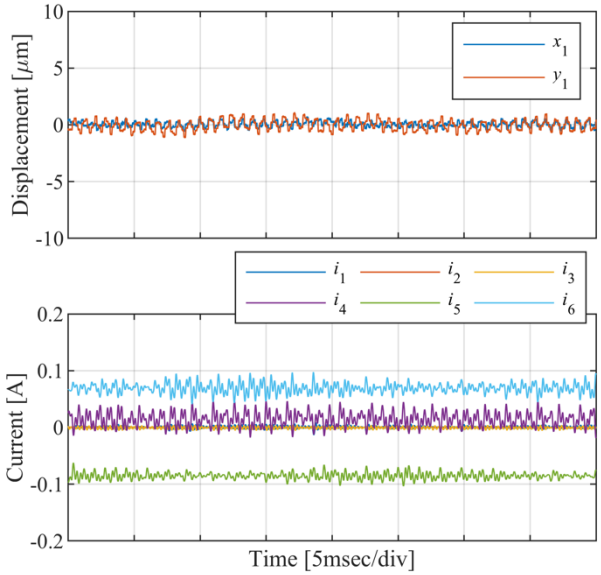

(a) AMB1 with current limit of 0.2 A

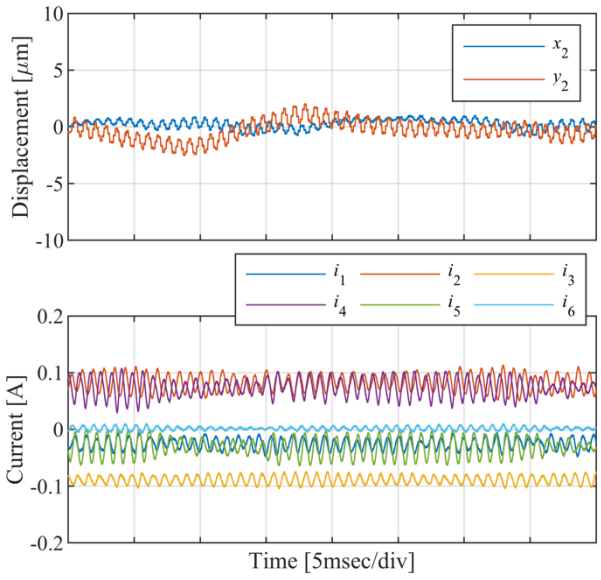

(b) AMB2 with current limit 0.1 A

Figure 10. Displacement and coil currens. P-, D- and I-gains were 17 N/mm, 0.025 Ns/mm and 10 N/mms, respectively.

IV. Conclusions

In this paper, we introduced a novel controller for 6-pole AMBs, which switches 3-coil and 5-coil modes to realize both low power consumption and large bearing force. The experimental results showed that the proposed method realizes stable levitation with lower current limit compared with other controllers.

References

[1] H. Kanebako and Y. Okada, New Design of Hybrid Type Self-Bearing Moor for High-Speed Miniature Spindle, Proceedings of The Eighth International Symposium on Magnetic Bearings, Mito, Japan, pp. 65-70, 2002.

[2] L. Li, T. Shinshi, J. Kuroki and A. Shimokohbe, A Simple and Miniaturized Magnetic Bearing for Cost-Sensitive Applications, Proceedings of The Eighth International Symposium on Magnetic Bearings, Mito, Japan, pp. 561-56, 2002.

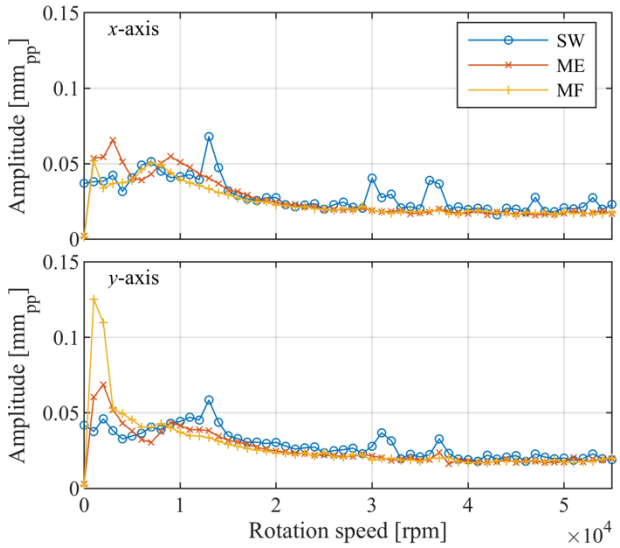

Figure 11. Amplitude of ocillation with switching controller (SW), minimum energy controller (ME) and maximum force controller (MF).

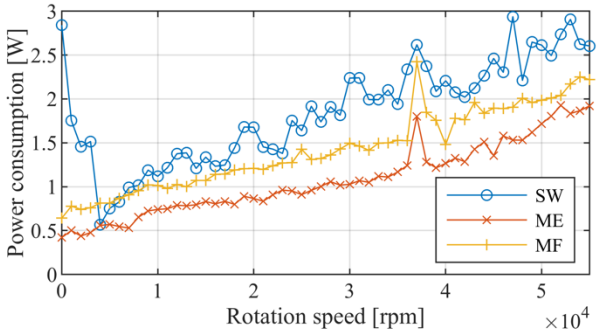

Figure 12. Power consumption.

[3] J. Asama, D. Watanabe, T. Oiwa and A. Chiba, Development of a One-Axis Actively Regulated Bearingless Motor with a Repulsive Type Passive Magnetic Bearing, Proceedings of The 2014 International Power Electronics Conference, Hiroshima, Japan, pp. 988-993, 2014.

[4] M. Osa, T. Masuzawa, T. Saito and E. Tatsumi, Magnetic levitation performance of miniaturized magnetically levitated motor with 5-DOF active control, Mechanical Engineering Journal, Vol. 4, No, 5, Paper No. 17-00007, 2017.

[5] S. Ueno, T. Arai and K. Odagiri, Control of an Active Magntic Bearing with 6 Concentrated Wound Poles Using Bias Current, Jouranl of the Japan Society of Applied Electromagnetics and Mechanics, Vol. 12, No. 1, pp. 54-61, 2004 in Japanese.

[6] T. Yoshida, S. Ueno, Y. Okada, T. Arai and K. Odagiri, Linearization Control of 3 Pole Internal PM Type Hybrid Magnetic Bearings, Jouranl of the Japan Society of Applied Electromagnetics and Mechanics, Vol. 14, No. 4, pp. 406-412, 2006 in Japanese.

[7] S. Ueno, T. Arai and K. Odagiri, Minimum Energy Control of 6 Salient-pole Type Active Magnetic Bearing, Jouranl of the Japan Society of Applied Electromagnetics and Mechanics, Vol. 15, No. 1, pp. 34-41, 2007 in Japanese.

[8] S. Ueno, Maximum Bearing Force Control for 6 Salient-Pole Active Magnetic Bearings, Transactions of the Japan Society of Mechanical Engineers, Series C, Vol. 79, No. 801, pp. 1475-1482, 2013 in Japanese.

[9] H. Sakai and S. Ueno, Rotation Tests of 6 Salient-Pole Active Magnetic Bearings, Proceedings of The 12th International Conference on Motion and Vibration, Sapporo, Sapporo, Japan, 2014.

[10] M. Chiba, S. Ueno and C. Jiang, Performance comparison of 6 Salient-Pole Active Magnetic Bearings by the defferece in the control method, Jouranl of the Japan Society of Applied Electromagnetics and Mechanics, Vol. 25, No. 2, pp. 174-179, 2017 in Japanese.